Journal of Hazardous Materials 203–204 (2012) 151–157

Contents lists available at SciVerse ScienceDirect

Journal of Hazardous Materials

journal homepage: www.elsevier.com/locate/jhazmat

One-step preparation of CdS nanocrystals supported on thiolated silica-gel matrix and evaluation of photocatalytic performance

George R.S. Andrade[a], Cristiane C. Nascimento[a], Erick C. Neves[b], Cintya D'Angeles Espirito Santo Barbosa[c], Luiz P. Costa[d], Ledjane S. Barreto[a,b], Iara F. Gimenez[a,c,*]

[a] Programa da Pós-graduação em Ciência e Engenharia de Materiais, Universidade Federal de Sergipe, Av. Marechal Rondon s/n, Cidade Universitária "Prof. José Aloísio de Campos", CEP 491000-000, São Cristóvão, SE, Brazil

[b] Núcleo de Ciência e Engenharia de Materiais, Universidade Federal de Sergipe, Av. Marechal Rondon s/n, Cidade Universitária "Prof. José Aloísio de Campos", CEP 491000-000, São Cristóvão, SE, Brazil

[c] Núcleo de Pos-graduação em Química, Universidade Federal de Sergipe, Av. Marechal Rondon s/n, Cidade Universitária "Prof. José Aloísio de Campos", CEP 491000-000, São Cristóvão, SE, Brazil

[d] Institute of Chemistry, University of Campinas – UNICAMP, P.O. Box 6154, 13083-970 Campinas, SP, Brazil

ARTICLE INFO

Article history:
Received 26 August 2011
Received in revised form
28 November 2011
Accepted 29 November 2011
Available online 7 December 2011

Keywords:
CdS quantum dots
Organofunctionalized silica
Photoluminescence
Photocatalysis
Dyes

ABSTRACT

Here we report the use of a thiol-functionalized silica-gel to prepare supported CdS nanocrystals by a facile one-step procedure. Upon changing the relative proportion of the matrix we obtained nanocrystals with different average sizes and size distributions, as evidenced by spectroscopic measurements as well as TEM images. Photoluminescence spectra also indicated that the main effect of the matrix is related to the size control since the spectral profiles were found to be strongly dependent on the excitation wavelength. The performance of the material in the photocatalytic degradation of two commercial dyes (methylene blue and rhodamine 6G) has been tested under sunlight radiation, showing promising results. Almost complete decolorization has been observed after 80 min of exposure, with no adsorption on the silica surface.

1. Introduction

Nanocrystalline cadmium sulfide (CdS) and other semiconductor nanocrystals are attractive in diverse research contexts owing to well-established preparation methods and controllable properties such as visible-light photoluminescence [1,2]. Several methods were reported to control the size, shape and consequently the properties of semiconductor nanocrystals. The use of organometallic precursors [3], capping agents, reverse micelles [4,5], *etc.* has been reported aiming to obtain particles with controllable morphologies and electronic as well as photophysical properties.

Considering potential applications, the deposition or immobilization of CdS particles as well as other semiconductors is crucial to open the possibility of obtaining devices. Moreover this can also provide a means of controlling the sizes and stabilizing the nanoparticles into solid matrices [6]. In this context, semiconductor nanocrystals have been anchored on solid materials such as different types of clays [7], graphene [8], carbon nanotubes [9] silica xerogels [6], zeolites [10] and other mesoporous matrices [11], *etc.* In general the particles are prepared previously by methods such as reverse micelles and immobilized in a second step [12]. In a different approach CdS nanocrystals are prepared *in situ* over the surface or within the pores of silica supports such as glasses, xerogels, thin films and also zeolites [13]. Alternatively the nanocrystals can be pre-formed by colloidal chemistry methods using 3-(mercaptopropyl)trimethoxysilane as capping agent taking advantage of the ability of the ligand to participate in the sol–gel process, which can be described as the *in situ* preparation of the support [14]. On the other hand, the generation of specific binding sites via chemical modifications of the support may provide a means of controlling the morphological features of the anchored particles. Thiolated silica-gels such as those described by Walcarius et al. [15] and Vieira et al. [16] in the context of metal ion adsorption have not been studied in the present context despite potential advantages such as ease of preparation and suitable morphological control of nanocrystals. So here we propose the study of a thiolated silica-gel in the size and morphological control of CdS nanocrystals as well as the photocatalytic application of the resulting material.

One of the most popular applications of semiconductor nanocrystals is in the photocatalytic degradation of pollutants [17].

* Corresponding author.
E-mail address: gimenez@ufs.br (I.F. Gimenez).

0304-3894/$ – see front matter © 2011 Elsevier B.V. All rights reserved.
doi:10.1016/j.jhazmat.2011.11.086

Dyes are suitable candidates for this kind of study since they are extensively used in textile, paper, plastic and other industries, being discharged in the environment and causing several problems [18]. The process of photocatalysis is included among the advanced oxidative processes in which reactive species such as hydroxyl radicals are generated and participate in the degradation of pollutants [19]. The photocatalysis with semiconductor nanocrystals has been reviewed previously [20,21]. TiO_2 is considered the ideal photocatalyst in terms of activity and advantages such as harmlessness [22] but as its band gap is in the UV region, TiO_2 absorbs only a small fraction of sunlight. Other semiconductors such as CdS absorb visible light being suitable for applications with sunlight, however suffer from drawbacks such as toxicity, and lack of durability in some pH values, *etc.* [23]. Additionally supported nanocrystals are studied to overcome the difficulties in recovering the photocatalysts at the end of the process when colloidal suspensions are used. In summary, those are some of the reasons why there is a great deal of effort in the search for new photocatalysts.

Here we examined the possibility of obtaining CdS nanocrystals *in situ* in thiol-modified silica matrices. Microstructural and photoluminescence properties as well as the possibility of application as photocatalyst were studied.

2. Experimental

2.1. Materials

In this work the following reagents and solvents were used as received: Silica gel 60 (Vetec), 3-(mercaptopropyl)trimethoxysilane (MPTMS) (Merck), cadmium acetate (Acros Organics), thiourea (Acros Organics), toluene (Isofar), dimethylformamide (DMF) (Vetec), acetone (Cromoline) Rhodamine 6G (R6G) was purchased from Merck and methylene blue (MB) (C.I. 52015) was a gift from the Santista Textiles Industries (Sergipe/Brazil), provided by the Dystar Dyes Company. All solutions were prepared with ultrapure water generated by a MILLI-Q purification system.

2.2. Preparation of the thiolated silica matrix–mercaptopropyl silica (MPS)

The silica-gel functionalization has been performed according to the procedure reported by Walcarius et al. [15]. In a typical procedure, 5 mL of MPTMS were added to 50 mL of a toluene suspension containing 5 g of silica-gel. The mixture was refluxed for 24 h under constant stirring. The product was filtered, washed with toluene and dried in an oven at 45 °C for 12 h. The product was characterized by FTIR measurements (not shown) of KBr pellets in a PerkinElmer Spectrum BX with 4.0 cm^{-1} resolution.

2.3. Preparation of MPS/CdS samples

Different MPS masses were added (150 mg, 200 mg and 250 mg) to 25 mL of a DMF solution containing 20 mmol L^{-1} cadmium acetate and 37.5 mmol L^{-1} thiourea, followed by heating at 135 °C for 10 min. The resulting yellow solids were filtered, washed with approximately 50 mL acetone three consecutive times and dried in an oven at 45 °C for 12 h. Samples were nominated S150, S200 and S250 on the basis of the MPS mass used. Samples were characterized by UV/visible reflectance spectroscopy using an Ocean Optics HR2000 spectrophotometer coupled to an integrating sphere. Photoluminescence (PL) spectra were acquired with an ISS/PC1 Photon Counting Spectrofluorimeter equipped with a 30 W Xe lamp and 2 mm slits. XRD powder patterns were measured with a Rigaku RINT 2000/PC with a Cu-Kα (λ = 1.5418 Å) operating at 40 kV/40 mA, in continuous mode with 2°/min scanning rate.

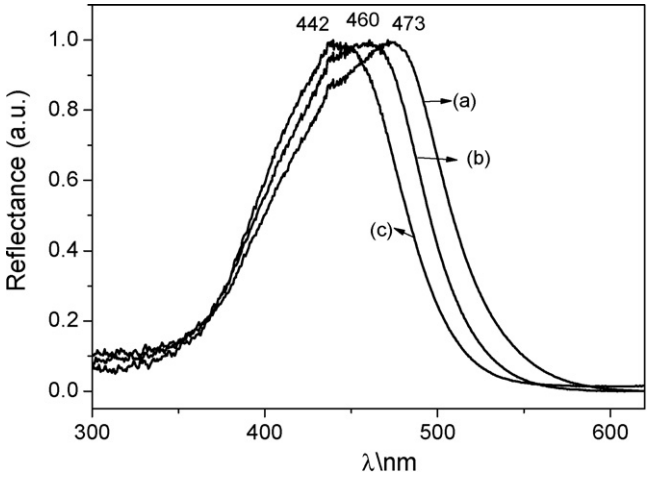

Fig. 1. UV/visible reflectance spectra for MPS/CdS samples being: (a) S150, (b) S200, (c) S250.

Transmission Electron Microscopy (TEM) images were obtained using TEM-MSC-JEOL 2100 microscope at an accelerating voltage of 200 kV. Samples for TEM observation were prepared by dropping an isopropanol suspension of the wet nanocomposite onto a carbon-coated copper grid and allowing the solvent to evaporate at 80 °C in vacuum.

3. Photocatalysis tests

The S250 sample has been chosen as the support for photocatalysis tests since this sample exhibited the smaller CdS nanocrystals. For the experiments, 50 mg of this sample were added to 20 mL of a 0.31 mmol L^{-1} of MB aqueous solution and to 20 mL of a 0.21 mmol L^{-1} R6G aqueous solution, in 125 mL conical flasks coupled to stopcock adapters. In both cases the suspensions were initially stirred for 20 min in dark conditions prior to sunlight irradiation, in order to ensure initial adsorption on the semiconductor surface. After this time interval the exposure to sunlight was started, under constant stirring using a multipoint magnetic stirrer. Aliquots were taken up every 5 min and used, after centrifugation, for UV/visible measurements in a PerkinElmer Lambda 45 spectrophotometer for the determination of the concentration of the dyes. Experiments were conducted in triplicate in daytime hours varying from 13:00 h–15:00 h when the sunlight intensity fluctuations are negligible. Meteorological data indicated that the region is subject to an average radiant exposure of 2900 kJ m^{-2} at the time of experiments. Chemical oxygen demand evaluation of the solutions after 80 min exposure was carried out using standard methods [24]. The Cd^{2+} concentration in the liquid phase after the photocatalysis tests was performed in duplicate by atomic absorption measurements using a Varian FS 220 spectrophotometer.

In order to properly quantify the role of adsorption of the dyes on the silica matrix, an analogous set of experiments was carried out protected from light for the same total time interval of the photocatalysis experiments. Data acquired from those tests were designated as “adsorption experiments”.

4. Results and discussion

Here we evaluated the spectroscopic properties, the crystalline phases present and morphological features of CdS nanocrystals supported on thiolated silica. Optical reflectance spectra are shown in Fig. 1, exhibiting a blue shift of the maximum absorption wavelength with increasing the relative proportion of the matrix. This can be related to a decrease in the average size of the particles,

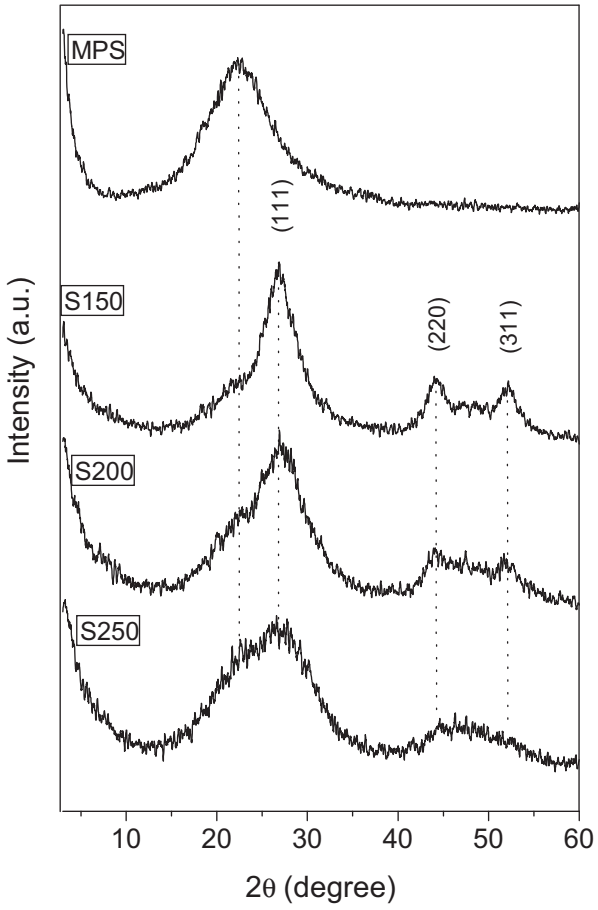

Fig. 2. Powder XRD patterns for: MPS and different MPS/CdS samples.

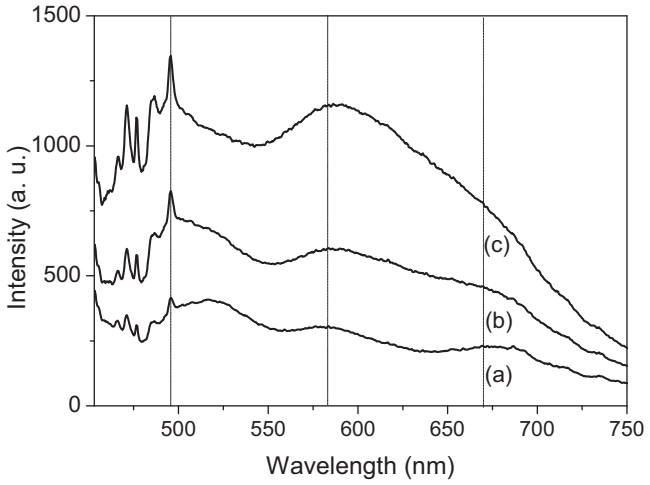

Fig. 3. Photoluminescence spectra measured with excitation wavelength 425 nm for MPS/CdS samples being: (a) S150, (b) S200, (c) S250.

as a result of the dependence of the electronic structure with the nanocrystal size [25]. The band gap energy – which is dependent on the nanocrystal size – determines the threshold energy for an electronic transition in a semiconductor nanocrystal [26]. Also the bandwidth decreased with increasing matrix proportion, which may be related to a lower dispersion of sizes. As size dispersion increases the bands in general become broader and less defined. This is confirmed by size estimations made from TEM images: 6–8 nm (S150); 4.5 nm (S200) and 4.0 nm (S250) (see discussion on TEM images).

The band gaps calculated from the effective mass approximation for S150, S200 and S250 were 2.62 eV, 2.71 eV and 2.81 eV, respectively. This variation can be related to the decrease in the average sizes. The band gap energy for bulk CdS is 2.42 eV and its optical absorption is observed near 512 nm [27]

The samples were also characterized by powder XRD measurements, Fig. 2. The diffraction pattern of mercaptopropyl silica is characterized by an amorphous halo centered at $2\theta = 22^{\circ}$. Samples containing CdS exhibited, in addition to this halo, broad peaks around at $2\theta = 26.7^{\circ}$, 44.2°, and 51.8°. Those peaks can be assigned respectively to planes 1 1 1, 2 2 0 and 3 1 1 of the cubic zinc blend phase of CdS in agreement to literature data [28]. As the relative proportion of the matrix increased, the peak width also increased probably as a result of the reduction of particle sizes. However owing to interference of the amorphous pattern of the matrix, it was not possible to estimate the particle sized by Scherrer's Law.

PL spectra of the three samples are all characterized by two distinct emission regions: the intrinsic recombination mechanism in the range 400–550 nm and recombination in surface trap defects in 550–700 nm [29]. Here we observed a fine structure in the direct recombination region, which has been described as a result of the excitation energy being insufficient to excite the whole sample, as there is size dispersion and consequently a dispersion of the band gap energy [30]. In Fig. 3 all spectra were measured upon excitation at 425 nm which probably excited different fractions of nanocrystals present in each sample, accounting for differences in the spectral profile for different samples. For instance the intensity of the intrinsic recombination bands for sample S150, specially the band at 517 nm, is higher than the intensity for the recombination in surface trap states. This can be understood considering that this sample contains larger particles for which the relative contribution of the surface is less significant in comparison with the other samples.

We also studied the dependence of the PL spectra with the excitation energy for the different samples. Spectra obtained are shown in Fig. 4. In all cases the spectral profiles depended significantly on the excitation wavelength, probably due to an effect of size distribution in the samples. According to Murphy and co-workers [31] if all nanocrystals in a semiconductor sample had the same particle size the profile of the PL spectrum would not depend on the excitation energy, for energies equal or above the band gap. On the other hand, size dispersion makes necessary progressively higher excitation energies in order to excite all nanocrystals in the sample. If the excitation energy only excites the larger particles, the direct recombination band is favored over the recombination in surface states, which can progressively favored as higher energies are used for excitation [32]. In fact this has been observed for all samples studied and it also indicated that the silica matrix influenced the average sizes as well as the size distribution but failed in passivating the surface, otherwise we would observe a decrease in the contribution of surface defects as the matrix proportion increased. Moreover we observe a shift in the intrinsic recombination band at 510–535 nm with the excitation wavelength which confirms the size effect. This observation is clearer for S150 sample: the band position shifts from 511 nm to 537 nm. The band between 550 nm and 600 nm is barely affected but the band due to trap states moves from 685 nm to 650 nm indicating that the defect levels are also sensitive to particle size. Similar observations can be made for the other samples.

TEM images were acquired in order to confirm assumptions made from spectroscopic data and also to give a better understanding of the CdS distribution along the silica matrix. Fig. 5a shows an overview of S250 along with a zoom (Fig. 5b) highlighting a specific region on the surface. It can be verified that the CdS nanocrystals

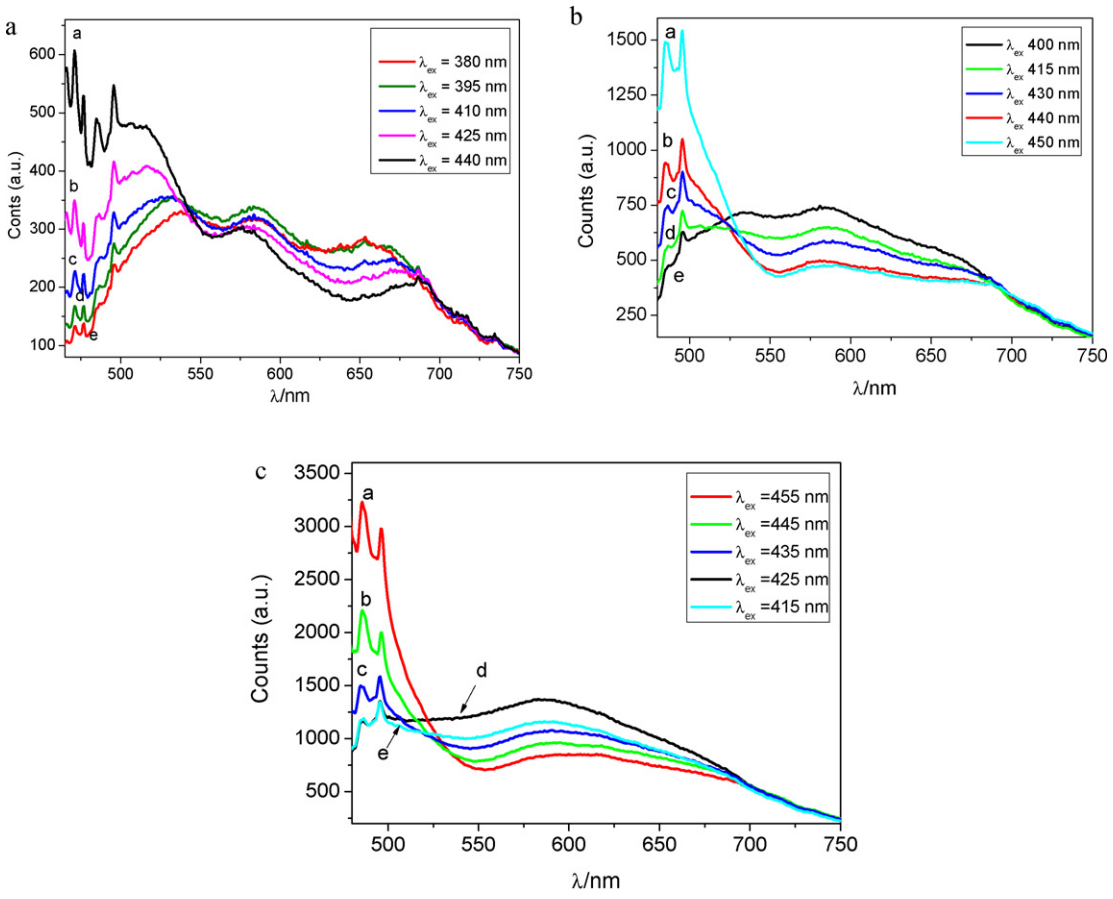

Fig. 4. Photoluminescence spectra measured with different excitation wavelengths for MPS/CdS samples being: (a) S150, (b) S200, (c) S250.

are uniformly distributed on the matrix in the form of high contrast points, although it is not possible to unequivocally confirm its presence inside the matrix porosity. The identification of the nanocrystals as the darker points along the matrix has been confirmed by the localization of such points over a thin border of the matrix, allowing the observations of CdS lattice fringes (see the following discussion).

For a proper evaluation of the effect of changing the proportion of the matrix relative to Cd^{2+} ions, Fig. 6a shows TEM images of the MPS matrix in comparison with CdS-containing samples. The morphology of the matrix is characterized by an irregular external shape and slightly darker regions due to thickness differences. For the samples containing CdS, the presence of nearly spherical darker points throughout the matrix is evident. Fig. 6b shows a very thin border of the matrix containing the high contrast points, in which the presence of lattice fringes is evident. A crude attempt to measure the lattice distance gave values close to 0.35–0.4 Å, which are close to values assigned to CdS [6]. Considering the samples prepared with different proportions of the matrix, significant size dispersion is observed for all samples. An accurate analysis of size distribution was not possible for two reasons. First the interference of the matrix makes it difficult to properly observe

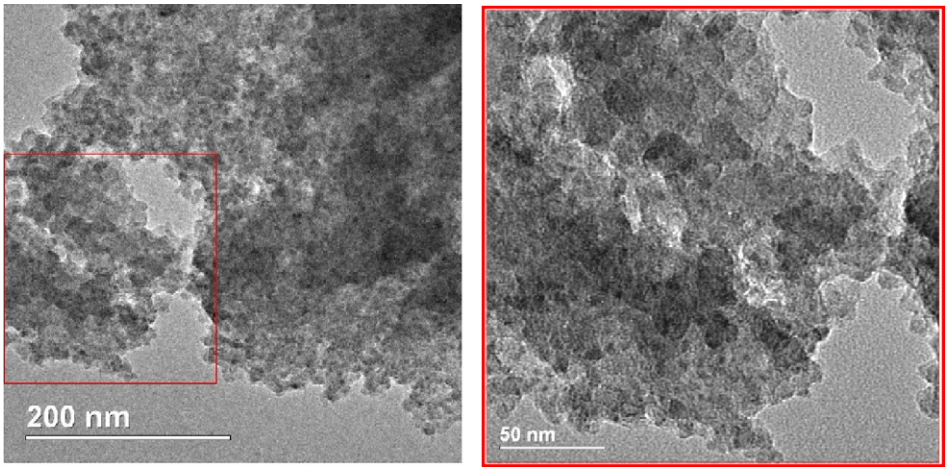

Fig. 5. TEM images for sample S250 showing: (a) an overview of the surface of this sample; (b) a zoom of the highlighted region in Fig. 5a.

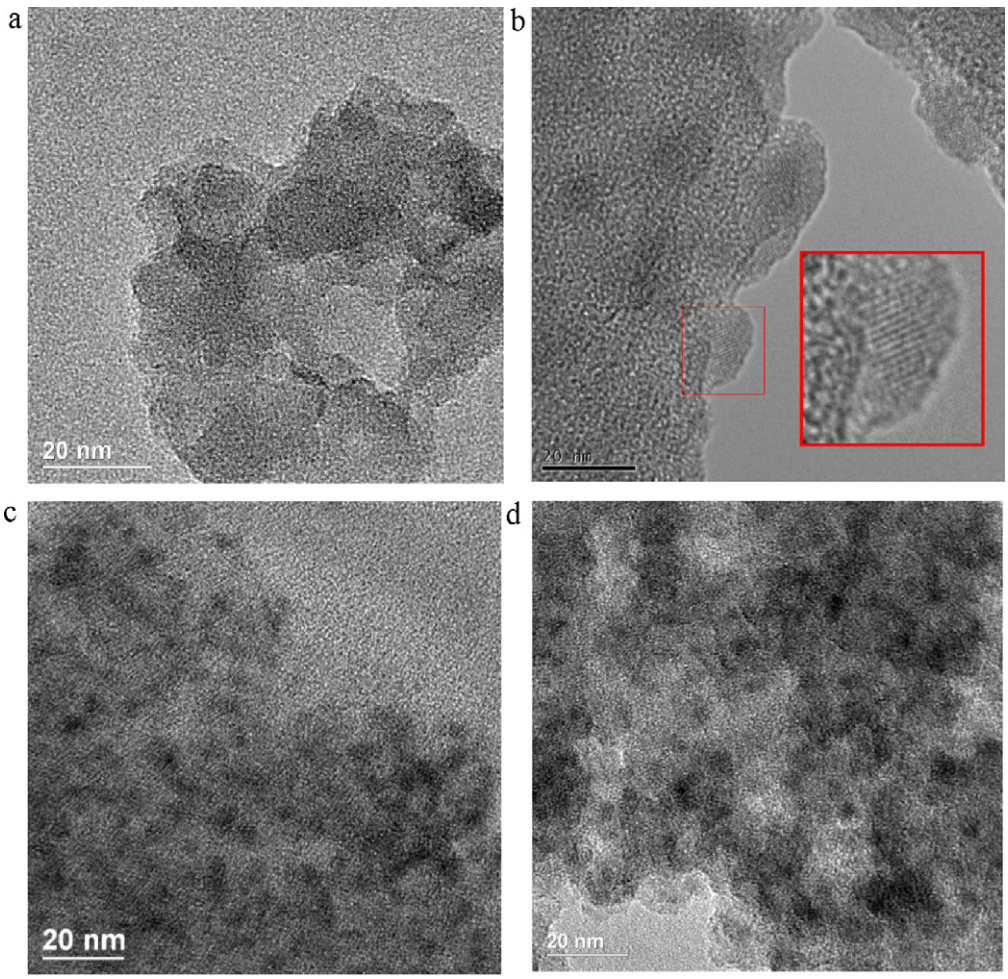

Fig. 6. TEM images for (a) MPS, (b) S150, (c) S200 and (d) S250.

the particle boundaries and second there is some superposition of image projections of nanocrystals probably present in different depths of the samples. However, it can be observed that there is a decrease in the overall particle sizes with the increase of matrix proportion. We did measure the diameters of some well-defined particles, estimating the presence of nanocrystals of 6–8 nm, 4.5 nm and 4.0 nm, respectively in sample S150, S200 and S250. This is an interesting result since it shows that the thiolated matrix is suitable to control morphological properties of the nanocrystals in a single-step preparation.

Finally the possibility of using the materials as photocatalysts for decolorization of dye solutions under sunlight exposure has been evaluated using MB and R6G. Fig. 7a and b shows the evolution of absorption spectrum of the dyes with the exposure time in the presence of the solids, showing that during a period of 80 min the intensity of the absorption bands continuously decrease until practically disappear. Percentage COD reduction after 80 min was 42% in the case of MB and 44% for R6G, respectively, indicating that although color removal was complete in both cases only partial mineralization has been achieved. In general several hours are necessary for higher mineralization degrees [33] and the values found lie in the range described for efficient photocatalysts. Attempts to identify reaction products failed probably owing to the presence of a complex mixture of products partially decomposed. Finally a leaching evaluation indicated the presence of 10 ppm Cd^{2+} after 80 min, which is lower than values observed in previous studies [34] but it is still well above recommended levels for drinking water, for instance.

Another observation is that concomitantly with the intensity decrease there is also a blue shift of the maximum absorption wavelength in both cases. For MB this is related with the formation of demethylated derivatives during the process [35]. After 80 min a very weakly intense spectrum shows a maximum at 617 nm which is related with a partially demethylated MB structure, probably present in a very low concentration. For R6G a more pronounced band shift is observed which have been attributed to the formation of N-deethylated derivatives [36]. It is interesting to note that the band shift which accompanies N-deethylation is not always observed in the course of photocatalytic studies of R6G [36]. It has been reported that this is a process that occurs at solid surfaces in contrast to degradation of the rhodamine chromophore, which predominates in the bulk of the solution [37]. Thus the band shift observed indicates that adsorption on the CdS surface even in a slight extent is an important step in the present case.

The adsorption onto the semiconductor surface is an important step of photocatalysis, but as we used a silica-gel derivative as support for QD preparation, it was necessary to evaluate the contribution of adsorption onto the silica matrix to the decolorization. Thus we carried out analogous experiments by stirring the same volume of solution with an equal mass of the solid under dark conditions and measuring the absorbance periodically. Fig. 7c and d compares the variation in the concentration for the two dyes studied with time for photocatalysis and adsorption experiments. It is clear that the contribution of adsorption is negligible in the time required for photodecolorization. Finally, photolysis tests (Supplementary Material) revealed that no change occurred under

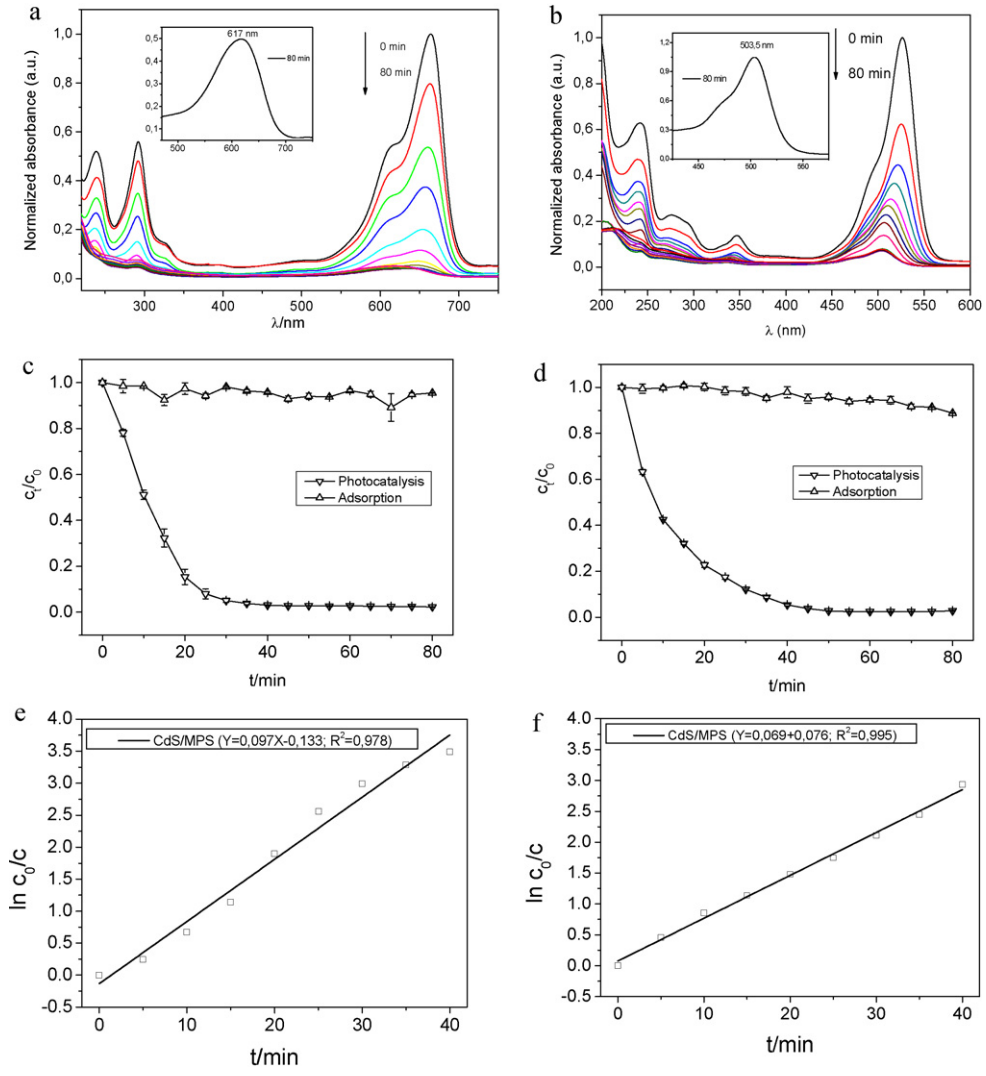

Fig. 7. Results of the photocatalysis tests: (a,b) evolution of the absorption spectra in solution with time during the photocatalysis (inset show the spectrum observed in the final measurement) for MB (a) and R6G (b); (c,d) comparison of the concentration rate relative to initial value at each time in the photocatalysis and adsorption experiments for MB (c) and R6G (d); (e,f) plots of the Langmuir–Hinshelwood kinetic model for MB (e) and R6G (f).

sunlight irradiation in the absence of the catalyst, confirming the role of photocatalysis. We also tested (Supplementary Material) CdS particles prepared without passivating agent in photocatalysis, observing a significantly lower decolorization degree.

A brief word comparing the photodegradation degree of the two different dyes, which have been found to be very similar, probably lie in the characteristics of the photocatalyst. MB and R6G belong respectively to thiazine and xanthene families, which are among the most studied dye categories in this context, as reviewed by Rajeshwar et al. [17] indicating that both are suitable candidates for photodegradation.

Finally we used the variation of dye concentration with time to verify if our data obeyed the Langmuir–Hinshelwood kinetic model, which is widely used to adjust kinetic data from reaction occurring at surfaces [17,20]. Briefly, this model is used on the basis of the following assumptions: (i) as a heterogeneous process, the reaction rate depends in principle on the surface coverage of all reactants, but it can be assumed that this parameter varies significantly only for the pollutant being degraded; (ii) the concentration of the dye in the liquid phase is significantly lower than its maximum possible value. In this case, the process can be described by a pseudo-first order kinetic model [20]. The plots of $\ln(C/C_0)$ versus time (Fig. 7e and f), where C_0 is the initial dye concentration and C is the concentration remaining after each time interval showed a linear behavior for both dyes with rate constants of 0.0971 min^{-1} and 0.0693 min^{-1} for MB and R6G respectively.

5. Conclusions

The thiol-derivative of silica gel (MPS) can be used to successfully obtain CdS nanocrystals with the possibility varying the average diameter of the nanocrystals, by the use of different matrix/Cd^{2+} proportions. The resulting materials exhibited interesting optical properties as evidenced by the PL spectra and presented promising photocatalytic activity towards dye degradation under sunlight, according to the preliminary tests.

Acknowledgments

Authors are grateful to Brazilian funding agencies CNPq, Fapitec, Capes, for financial support. Contributions from LNNano-LME (Campinas-SP, Brazil) for TEM analysis are also gratefully acknowledged.

Appendix A. Supplementary data

Supplementary data associated with this article can be found, in the online version, at doi:10.1016/j.jhazmat.2011.11.086.

References

[1] N. Gaponik, S.G. Hickey, D. Dorfs, A.L. Rogach, A. Eychmuller, Progress in the light emission of colloidal semiconductor nanocrystals, Small 6 (2010) 1364–1378.
[2] V. Biju, T. Itoh, A. Sujith, M. Ishikawa, Semiconductor quantum dots and metal nanoparticles: syntheses, optical properties, and biological applications, Anal. Bioanal. Chem. 391 (2008) 2469–2495.
[3] C.B. Murray, D.J. Norris, M.G. Bawendi, Synthesis and characterization of nearly monodisperse CdE (E = S, Se, Te) semiconductor nanocrystallites, J. Am. Chem. Soc. 115 (1993) 8706–8715.
[4] M.P. Pileni, Nanosized particles made in colloidal assemblies, Langmuir 13 (1997) 3266–3276.
[5] L.H. Yuwen, B.Q. Bao, G. Liu, J. Tian, H.T. Lu, Z.M. Luo, X.R. Zhu, F. Boey, H. Zhang, L.H. Wang, One-pot encapsulation of luminescent quantum dots synthesized in aqueous solution by amphiphilic polymers, Small 2 (2011) 1456–1463.
[6] H. El Hamzaoui, R. Bernard, A. Chahadih, F. Chassagneux, L. Bois, D. Jegouso, L. Hay, B. Capoen, M. Bouazaoui, Laser-induced direct space-selective precipitation of CdS nanoparticles embedded in a transparent silica xerogel, Nanotechnology 21 (2010) 134002–134010.
[7] P. Praus, O. Kozak, K. Koci, A. Panacek, R. Dvorsky, CdS nanoparticles deposited on montmorillonite: preparation, characterization and application for photoreduction of carbon dioxide, J. Colloid Interface Sci. 360 (2011) 574–579.
[8] C. Nethravathi, T. Nisha, N. Ravishankar, C. Shivakumara, M. Rajamathi, Graphene – nanocrystalline metal sulphide composites produced by a one-pot reaction starting from graphite oxide, Carbon 47 (2009) 2054–2059.
[9] B.H. Juarez, M. Meyns, A. Chanaewa, Y. Cai, C. Klinke, H. Weller, Carbon supported CdSe nanocrystals, J. Am. Chem. Soc. 130 (2008) 15282–15284.
[10] E. Caponetti, L. Pedone, M.L. Saladino, D.C. Martino, G. Nasillo, MCM-41-CdS nanoparticle composite material: preparation and characterization, Microporous Mesoporous Mater. 128 (2010) 101–107.
[11] X. Du, J. He, Elaborate control over the morphology and structure of mercapto-functionalized mesoporous silicas as multipurpose carriers, Dalton Trans. 39 (2010) 9063–9072.
[12] T. Hirai, H. Okubo, I. Komasawa, Incorporation of CdS nanoparticles formed in reverse micelles into silica matrices via a sol–gel process: preparation of nano-CdS containing silica colloids and silica glass, J. Mater. Chem. 10 (2000) 2592–2596.
[13] C. Mao, J. Qi, A.M. Belcher, Building quantum dots into solids with well-defined shapes, Adv. Funct. Mater. 13 (2003) 648–656.
[14] Y.-I. Wang, J.-P. Lu, X.-F. Huang, J.-X. Long, Z.-F. Tong, One step synthesis of silica-coated nanoparticles at room temperature and their luminescence properties, Mater. Lett. 62 (2008) 3413–3415.
[15] A. Walcarius, M. Etienne, J. Bessiere, Rate of access to the binding sites in organically modified silicates, Chem. Mater. 14 (2002) 2757–2766.
[16] E.F.S. Vieira, J.A. Simoni, C. Airoldi, Interaction of cations with SH-modified silica-gel: thermochemical study calorimetric titration and direct extent of reaction determination, J. Mater. Chem. 7 (1997) 2249–2252.
[17] K. Rajeshwar, M.E. Osugi, W. Chanmanee, C.R. Chenthamarakshan, M.V.B. Zanoni, P. Kajitvichyanukul, R. Krishnan-Ayer, Heterogeneous photocatalytic treatment of organic dyes in air and aqueous media, J. Photochem. Photobiol. C 9 (2008) 171–192.
[18] H. Zhu, R. Jiang, L. Xiao, Y. Chang, Y. Guan, X. Li, G. Zeng, Photocatalytic decolorization and degradation of Congo Red on innovative crosslinked chitosan/nano-CdS composite catalyst under visible light irradiation, J. Hazard. Mater. 169 (2009) 933–940.
[19] R. Andreozzi, V. Caprio, A. Insola, R. Marotta, Advanced oxidation processes (AOP) for water purification and recovery, Catal. Today 53 (1999) 51–55.
[20] J.-M. Herrmann, Photocatalysis fundamentals revisited to avoid several misconceptions, Appl. Catal. B: Environ. 99 (2010) 461–468.
[21] M.A. Fox, M.A. Dulay, Heterogeneous photocatalysis, Chem. Rev. 93 (1993) 341–357.
[22] A.L. Linsebigler, G. Lu, J.T. Yates Jr., Photocatalysis on TiO_2 surfaces: principles, mechanisms, and selected results, Chem. Rev. 95 (1995) 735–758.
[23] L.B. Reuterglrdh, M. Iangphasuk, Photocatalytic decolourization of reactive azo dye: a comparison between TiO_2 and CdS photocatalysis, Chemosphere 35 (1997) 585–596.
[24] APHA, Standard Methods for the Examination of Water and Wastewater, 19th ed., Am. Publ. Health Ass., 1995, 5550 p.
[25] A.M. Smith, S. Nie, Semiconductor nanocrystals: structure, properties and band gap engineering, Acc. Chem. Res. 43 (2010) 190–200.
[26] L.E. Brus, Electron-electron and electron-hole interactions in small semiconductor crystallites: the size dependence of the lowest excited electronic state, J. Chem. Phys. 80 (1984) 403–4409.
[27] K. Rajeshwar, N.R. Tacconi, C.R. Chenthamarakshan, Semiconductor-based composite materials: preparation, properties, and performance, Chem. Mater. 13 (2001) 2765–2782.
[28] C. Unni, D. Philip, S.L. Smitha, K.M. Nissamudeen, K.C. Gopachandran, Aqueous synthesis and characterization of CdS, CdS:Zn^{2+} and CdS: Cu^{2+} quantum dots, Spectrochim. Acta A 72 (2009) 827–832.
[29] N. de La Rosa-Fox, M. Pinero, R. Litran, L. Esquivias, Photoluminescence from CdS quantum dots in silica gel, J. Sol-Gel Sci. Technol. 26 (2003) 947–951.
[30] S. Okamoto, Y. Kanemitsu, H. Hosokawa, K. Murakoshi, S. Yanagida, Photoluminescence from surface-capped CdS nanocrystals by selective excitation, Solid State Commun. 105 (1998) 7–11.
[31] J.R. Lakowicz, I. Gryczynski, Z. Gryczynski, C.J. Murphy, Luminescence spectral properties of CdS nanoparticles, J. Phys. Chem. B 103 (1999) 7613–7620.
[32] S. Yang, W. Cai, H. Zeng, X. Xu, Ultra-fine b-SiC quantum dots fabricated by laser ablation in reactive liquid at room temperature and their violet emission, J. Mater. Chem. 19 (2009) 7119–7123.
[33] S.K. Kansal, M. Singh, D. Sud, Studies on photodegradation of two commercial dyes in aqueous phase using different photocatalysts, J. Hazard. Mater. 141 (2007) 581–590.
[34] A.H. Zyoud, N. Zaatar, I. Saadeddin, C. Ali, D. Park, G. Campet, CdS-sensitized TiO_2 in phenazopyridine photo-degradation: catalyst efficiency, stability and feasibility assessment, J. Hazard. Mater. 173 (2010) 18–325.
[35] M. Zaied, S. Peulon, N. Bellakhal, B. Desmazieres, A. Chaussé, Studies of N-demethylation oxidative and degradation of methylene blue by thin layers of birnessite electrodeposited onto SnO_2, Appl. Catal. B: Environ. 10 (2011) 441–450.
[36] T. Watanabe, T. Takirawa, K. Honda, Photocatalysis through excitation of adsorbates. Rhodamine B adsorbed to CdS, J. Phys. Chem. 81 (1977) 1845–1851.
[37] M.K. Seery, R. George, P. Floris, S.C. Pillai, Silver doped titanium dioxide nanomaterials for enhanced visible light photocatalysis, J. Photochem. Photobiol. A 189 (2007) 258–263.